J. Appl. Comput. Mech., 7(3) (2021) 1575-1582
DOI: 10.22055/JACM.2021.35350.2635

ISSN: 2383-4536
jacm.scu.ac.ir

Shahid Chamran University of Ahvaz

Journal of Applied and Computational Mechanics

Research Paper

On the Effect of the End-effector Point Trajectory on the Joint Jerk of the Redundant Manipulators

Xuan Bien Duong

Advanced Technology Center, Le Quy Don Technical University, Hoang Quoc Viet, Hanoi, 84, Vietnam

Received October 09 2020; Revised February 07 2021; Accepted for publication February 28 2021.
Corresponding author: X.B. Duong (duongxuanbien@lqdtu.edu.vn)

Abstract. This paper is focused on investigating the joints jerk of industrial serial redundant manipulators with 6 degrees of freedom (6-DOF) under the variation of the end-effector point (EEP) trajectory in the workspace. The EEP trajectories are initially built in the basic planes because of their simplicity, verification and experimentation are smooth, and most of the actual welded structures are performed on these basic planes. The jerk is determined by solving the inverse kinematics problem of the redundant system. This problem is solved based on the algorithm which is used for adjusting the increments of the generalized coordinate vector (AGV). The efficiency of this algorithm is shown through the error between a given trajectory and the recalculated trajectory through the forward kinematics problem. The result of this study allows us to evaluate the effect of the change of the trajectory on the kinematics characteristics of the robot in general and the jerk of the joints in particular. On the other hand, these results can be used as the basis for planning the EEP trajectory for redundant robots, developing algorithms to reduce joint jerky, increase the life of robot systems, and improve the accuracy of the redundant robot movement.

Keywords: Joint jerk, industrial robots, redundant system, end-effector point trajectory.

1. Introduction

In modern industrial production, automatic systems in general and industrial robots in particular are always oriented to achieve optimum performance. Flexibility, accuracy, load capacity, minimizing joint torque, and high-speed motion are factors that always improve system performance. For industrial robots, dexterity and flexibility are met based on the design of robots which have many degrees of freedom such as redundant manipulators as in [1-5].

Although the redundant system has plenty of advantages, there are also great challenges when considering this type of robot. The redundant manipulators have many links and types of joints which are linked together quite complicatedly making it difficult to modeling, kinematics and dynamics analyzing, and designing the control system. The major challenges are kinematics singularity, joint limitations, and obstacle avoidance in the workspace. The inverse kinematics problem (IK) and the control problem of the redundant robots are complicated because the calculation results of the IK are multi-solutions with kinematics singularities. If the IK algorithms do not handle the kinematics singularities and joint limitations well, the control system design problem will face a lot of difficulties in choosing the possible values, meeting the geometric constraints as well as the physical limitations of the system. Many algorithms are developed to solve the inverse kinematics problems such as Jacobian Transpose [6], Pseudoinverse [7], Damped Least Squares [8], Quasi-Newton, and conjugate gradient [9], [10], Closed-loop inverse kinematics [11-14]. The parallel genetic algorithm is used to solve the IK of the Puma 500 robot in [15]. The neutron network algorithm is used in [16], [17].

The control system is intelligently developed to ensure high precision. Improving the load capacity and acceleration of the robot depends heavily on the working conditions of the transmission system of the joints such as wear, jerk, vibration, joint clearance, etc. A system that has more degrees of freedom the more flexible the movement will be, avoiding singularity positions, avoiding obstacles [18], [19]. However, apart from the complex problem of the control system, the limitation and jerk of the joints also need to be considered. The evaluation of the influence of the varying trajectory on the joint jerk as a basis for designing the trajectory in accordance with the robot's characteristics has not been clearly considered. Jerk is quite important in the above factors because it is directly related to the wear and load capacity of the powertrain [20], [21]. Jerk is the time derivative of the acceleration and it is therefore related to the driving force of the system. Sudden jerk leads to actuator's wear, engendering resonant vibrations in the system structure. This makes it difficult for the control system to accurately monitor the motion state of the robot. The jerky of the EEP is investigated through the trajectory planning of the EEP in the workspace and it is considered in [22], [23]. The jerky of the joint is mostly mentioned by trajectory planning of joints in joint space and the derivative is continuous respect to time [20], [21], [24-29]. The problem of given the position, speed, acceleration and jerky of the EEP in the workspace to investigate the jerky of joints in the jointspace based on kinematics equations has not been specifically considered and it is just stopped at the level of accelerating joints [13], [30-33].

Published online: March 27 2021

Table 1. Kinematic parameters D-H

Links	D-H parameters			
	$\theta_i = q_i$	d_i	a_i	α_i
1	q_1	d_1	a_1	$\pi/2$
2	q_2	0	a_2	0
3	q_3	0	a_3	$\pi/2$
4	q_4	d_4	0	$\pi/2$
5	q_5	0	0	$-\pi/2$
6	q_6	d_6	0	0

The trajectory of the EEP directly affects the kinematics and dynamic behaviors of the robot joints. There are trajectories of the EEP that angle joints easily meet, but there are also the EEP trajectories that pose great challenges to accurately calculating the value of the joint angles to ensure movement requirements and fit the configuration physics of the robot. Furthermore, although the joint values assurances the above requirements, the values of acceleration and jerk have a great influence on the motion accuracy and the life of the actuators on the joints. Therefore, it is necessary to examine the effect of the EEP trajectory on the kinematics behavior of the robot in general and the jerk of the robot joints in particular. There are many studies on the EEP trajectory optimization with the minimum jerk or the shortest motion time. An algorithm to optimize the jerk in the time domain based on interval analysis is proposed in [24]. The trajectory time of a 7-DOF Kuka robot is optimized in [26] by building a control system with a given joint jerk input. The effects of torque, energy consumption, and jerk on the construction of a robot's collision avoidance trajectory in complex work environments are analyzed in [28]. The optimal trajectory design to minimize joint jerk contributes to improving the accuracy and increased travel speed for the robot are presented in [34], [35]. The algorithm for adjusting the collision avoidance for the robot and moving in the shortest time to the target is presented in [36]. Speed, acceleration, and jerk are used as input conditions of this adjustment algorithm. The jerk optimization of the robot with 7-DOF based on trajectory planning is described in [37]. The jerk is optimized in [38] based on toolpath design for redundant robots for 3D printing. There are many similar studies on this issue as can be seen in [39], [40], [41].

In this study, three trajectories in these basic planes are used to determine the joint jerk of a redundant manipulator with 6-DOFs fixed in a vertical plane. There are many different types of trajectories in space depending on the specific task and these are all based on the three basic planes. The position, velocity, acceleration, and jerk of the joints are the results of this problem. The inverse kinematics solving algorithm takes the given error of the joints variables and limits the joints as the conditions for performing the calculation. There are several reasons for choosing 3 basic planes for planning the EEP trajectory in the workspace. Firstly, this study is only at the beginning of the research on the joint's jerk of robots with simple and basic trajectories. Secondly, parameters of the EEP trajectories on these 3 planes can ensure bringing the EEP of the robot to the positions that is needed to be investigated such as the position outstretched, close to the robot's body, the position of rising or falling low close to the base. Thirdly, the EEP trajectories are easily built on these basic planes and easily verify reliability in both theoretical and experimental geometry calculations. On the other hand, easily fabricating auxiliary equipment such as jigs for experimenting, measuring, and verifying calculation results. Next, the analysis results of the problem in this paper can be used immediately because in reality most welded structures are mainly machined on these planes. Finally, the generalized EEP trajectory in the workspace can completely be built and investigated, but verifying the reliability and accuracy of the calculations will be a huge challenge, especially experimentally being verified. This paper is structured in 4 sections including Introduction, Materials and Methods, Simulation results and discussions, and finally Conclusion. Section 2 describes kinematics modeling the welding robot 6-DOF based multi-bodies system theory and DH method and analyzes the inverse kinematics problem using AGV algorithm. Section 3 presents the numerical simulation results which are calculated by MATLAB software.

2. Materials and methods

Consider the kinematics model and working range of industrial FD-V8 welding robot with 6-DOF as shown in Fig. 1. The fixed coordinate system is $(OXYZ)_0$ and $(OXYZ)_i$, (i = 1, ..., 6) are the local coordinate systems attached to link i. Table 1 describes the kinematic parameters according to the D-H rule [31]. Accordingly, with the transformation $\mathbf{H}_i$, (i = 1, ..., 6) homogeneous matrices are determined.

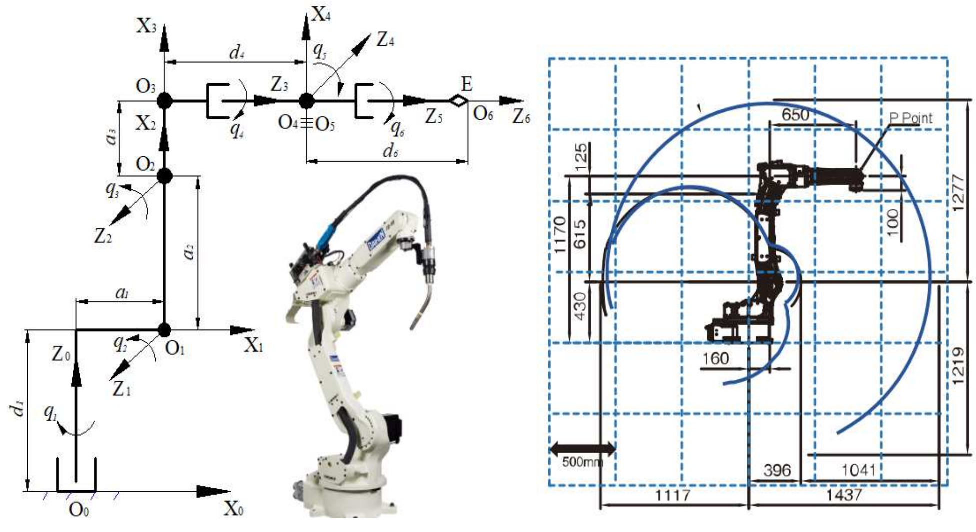

Fig. 1. Kinematic model of the industrial robot FD-V8 and the EEP working range [42]

The position of the EEP (point E in Fig. 1) following the fixed coordinate system is determined as follows [31]

$$\mathbf{D}_6 = \mathbf{H}_1\mathbf{H}_2\mathbf{H}_3\mathbf{H}_4\mathbf{H}_5\mathbf{H}_6 \tag{1}$$

The vector $\mathbf{q} = [q_1 \quad q_2 \quad q_3 \quad q_4 \quad q_5 \quad q_6]^T$ is the generalized coordinate vector. The forward kinematics equations are present as follows

$$\mathbf{x} = f(\mathbf{q}), \mathbf{x} \in \mathbf{R}^3, \mathbf{q} \in \mathbf{R}^6 \tag{2}$$

where $f(\mathbf{q})$ is a vector function representing the robot forward kinematics. Derivative eq. (2):

$$\dot{\mathbf{x}} = \mathbf{J}(\mathbf{q})\dot{\mathbf{q}} \tag{3}$$

where $\mathbf{J}(\mathbf{q})$ is the Jacobian matrix with size 3×6. The acceleration of the EEP can be given by derivation eq. (3) [13], [31], [33]

$$\ddot{\mathbf{x}} = \mathbf{J}(\mathbf{q})\ddot{\mathbf{q}} + \dot{\mathbf{J}}(\mathbf{q})\dot{\mathbf{q}} \tag{4}$$

Derivative eq. (4), the jerk of the EEP is determined as [30], [32]

$$\dddot{\mathbf{x}} = \mathbf{J}(\mathbf{q})\dddot{\mathbf{q}} + 2\dot{\mathbf{J}}(\mathbf{q})\ddot{\mathbf{q}} + \ddot{\mathbf{J}}(\mathbf{q})\dot{\mathbf{q}} \tag{5}$$

The inverse kinematics equations are determined as follows

$$\mathbf{q}(t) = f^{-1}(\mathbf{x}(t)) \tag{6}$$

However, due to the fact that the robot is a redundant system, solving the system of eq. (6) will give countless answers. Choosing the most suitable answer is a quite difficult problem. Therefore, building an effective algorithm to solve the problem of inverse kinetics is always interested in. Once the values of $\mathbf{q}$ have been determined from eq. (3), the joint velocities are calculated as

$$\dot{\mathbf{q}} = \mathbf{J}^{+}(\mathbf{q})\dot{\mathbf{x}} \tag{7}$$

where, $\mathbf{J}^{+}(\mathbf{q})$ is the pseudo-inverse matrix of $\mathbf{J}(\mathbf{q})$ and defined as [31]

$$\mathbf{J}^{+}(\mathbf{q}) = \mathbf{J}^{T}(\mathbf{q})\left[\mathbf{J}(\mathbf{q})\mathbf{J}^{T}(\mathbf{q})\right]^{-1} \tag{8}$$

the AGV algorithm [43] is applied to find $\mathbf{q}(t)$ value with given rules $\mathbf{x}_d(t), \dot{\mathbf{x}}_d(t), \ddot{\mathbf{x}}_d(t), \dddot{\mathbf{x}}_d(t)$. Assume redundant manipulator works in the period from $t = 0$ to $t = T$. Divide the robot working time into N equal intervals with $\Delta t = T/N$ and $t_{k+1} = t_k + \Delta t; k = 0,1,2,..N-1$. Implement the Taylor's expansion by ignoring infinitely small of order greater than or equal to 2 and use eq. (7) for $\mathbf{q}(t_{k+1})$ vector:

$$\mathbf{q}(t_{k+1}) = \mathbf{q}(t_k + \Delta t) = \mathbf{q}(t_k) + \dot{\mathbf{q}}(t_k)\Delta t + \frac{1}{2}\ddot{\mathbf{q}}(t_k)(\Delta t)^2 + ... = \mathbf{q}(t_k) + \mathbf{J}^{+}(\mathbf{q}(t_k))\dot{\mathbf{x}}(t_k)\Delta t \tag{9}$$

For simplicity, it is assumed that $\mathbf{q}(t_k) = \mathbf{q}_k, \dot{\mathbf{q}}(t_k) = \dot{\mathbf{q}}_k, \ddot{\mathbf{q}}(t_k) = \ddot{\mathbf{q}}_k, \dddot{\mathbf{q}}(t_k) = \dddot{\mathbf{q}}_k, \mathbf{x}(t_k) = \mathbf{x}_k, \dot{\mathbf{x}}(t_k) = \dot{\mathbf{x}}_k, \ddot{\mathbf{x}}(t_k) = \ddot{\mathbf{x}}_k, \dddot{\mathbf{x}}(t_k) = \dddot{\mathbf{x}}_k$. Also, assume that the approximate value $\mathbf{q}_0$ is known by the geometric or experimental method. Consider approximate value $\tilde{\mathbf{q}}_{k+1}$ as follows

$$\tilde{\mathbf{q}}_{k+1} = \mathbf{q}_k + \mathbf{J}^{+}(\mathbf{q}_k)\dot{\mathbf{x}}_k\Delta t \tag{10}$$

Determining the exact value of the generalized coordinate vector $\mathbf{q}_{k+1}$ yields

$$\Delta\mathbf{q}_{k+1} = 0 \tag{11}$$

The increment $\Delta\mathbf{q}_{k+1}$ needs to be determined. Perform Taylor's expansion for $\mathbf{x}_{k+1}$ from the forward kinematics equations (2) as follows

$$\mathbf{x}_{k+1} = f(\mathbf{q}_{k+1}) = f(\tilde{\mathbf{q}}_{k+1} + \Delta\mathbf{q}_{k+1}) = f(\tilde{\mathbf{q}}_{k+1}) + \mathbf{J}(\tilde{\mathbf{q}}_{k+1})\Delta\mathbf{q}_{k+1} + ... \tag{12}$$

So,

$$\Delta\mathbf{q}_{k+1} = \mathbf{J}^{+}(\tilde{\mathbf{q}}_{k+1})[\mathbf{x}_{k+1} - f(\tilde{\mathbf{q}}_{k+1})] \tag{13}$$

Then,

$$\tilde{\mathbf{q}}_{k+1} = \tilde{\mathbf{q}}_{k+1} + \Delta\mathbf{q}_{k+1} \tag{14}$$

If $|\Delta\mathbf{q}_{k+1}| \geq \varepsilon$ (where ε is the given joint error) then replace eq. (14) into eq. (13) and calculate eq. (13) until $|\Delta\mathbf{q}_{k+1}| < \varepsilon$ and determine the final value of $\mathbf{q}_{k+1}$ vector as follows

$$\mathbf{q}_{k+1} = \tilde{\mathbf{q}}_{k+1} \tag{15}$$

The velocity vector $\dot{\mathbf{q}}_{k+1}$ can be achieved from eq. (7). The values of $\mathbf{q}_{k+1}$ vector is tested under the following conditions

$$|\mathbf{q}_{k+1}| \leq \mathbf{q}_{\max} \tag{16}$$

where $\mathbf{q}_{\max}$ is the values of the joint position limit of the redundant robot FD-V8.

$$\mathbf{q}_{\max} = [q_{1\max} \quad q_{2\max} \quad q_{3\max} \quad q_{4\max} \quad q_{5\max} \quad q_{6\max}]^T \tag{17}$$

After condition (16) is assured, the robot's acceleration and jerk can be determined by eq. (7) with the above-mentioned values of $\mathbf{q}_{k+1}$ and $\dot{\mathbf{q}}_{k+1}$ vectors. if (16) is not met with joint $i (i = 1,..,6)$ such as $|(q_i)_{k+1}| > q_i^{\max}$ then $(\Delta q_i)_{k+1} = 0$ [44]. The $\mathbf{q}_{k+1}$ value is recalculated from eq. (11). The value of joint acceleration can be obtained from derivative eq. (7) with respect to time as follows

Table 2. Trajectories in the workspace

Trajectory	$x_E(m)$	$y_E(m)$	$z_E(m)$
Case 1	$0.7+0.3\sin(2t)$	$0.3\cos(2t)$	0.45
Case 2	0.7	$0.3\cos(2t)$	$0.65+0.3\sin(2t)$
Case 3	$1.075+0.3\sin(2t)$	0	$0.81+0.3\cos(2t)$

$$\ddot{\mathbf{q}}_{k+1}=\dot{\mathbf{J}}^{+}(\mathbf{q}_{k+1},\dot{\mathbf{q}}_{k+1})\dot{\mathbf{x}}_{k+1}+\mathbf{J}^{+}(\mathbf{q}_{k+1})\ddot{\mathbf{x}}_{k+1} \tag{18}$$

Similarly, the joint jerk is also determined from derivative eq. (18) with respect to time as follows

$$\dddot{\mathbf{q}}_{k+1}=\ddot{\mathbf{J}}^{+}(\mathbf{q}_{k+1},\dot{\mathbf{q}}_{k+1},\ddot{\mathbf{q}}_{k+1})\dot{\mathbf{x}}_{k+1}+2\dot{\mathbf{J}}^{+}(\mathbf{q}_{k+1},\dot{\mathbf{q}}_{k+1})\ddot{\mathbf{x}}_{k+1}+\mathbf{J}^{+}(\mathbf{q}_{k+1})\dddot{\mathbf{x}}_{k+1} \tag{19}$$

The position error $\mathbf{e}_{\mathbf{x}}$ of the EEP can be determined as follows

$$\mathbf{e}_{\mathbf{x}}=\mathbf{x}_d-f(\mathbf{q}) \tag{20}$$

All steps of the algorithm are described in Fig. 2.

3. Simulation results and discussion

The geometry parameters of the robot FD-V8 are presented as [42] $d_1=0.43(m), a_1=0.16(m), a_2=0.615(m), a_3=0.125(m)$, $a_3=0.125(m), d_4=0.65(m), d_6=0.475(m)$. The limit values of velocity is given as $\mathbf{q}_{\max}=[2.97\quad 2.7\quad 2.97\quad 3.14\quad 4.01\quad 6.28]^T(rad)$. The allowable error of joint variables in the algorithm is $\varepsilon=10^{-5}(rad)$. Given the trajectories of the EEP in three cases are shown in Tab. 2.

The numerical simulation results of case 1 with the trajectory in the workspace, the value of joint variables and simulation model in MATLAB are described respectively in Fig. 3, Fig. 4, and Fig. 5. Similar, simulation results of case 2 are shown in Fig. 6, Fig. 7, and Fig. 8. Case 3 is determined in Fig. 9, Fig. 10, and Fig. 11, respectively.

Fig. 12, Fig. 13, and Fig. 14 present the position error of the EEP between desired and calculated trajectories on axes OX, OY, and OZ respectively with 3 cases. The calculated positions are determined through solving forward kinematics problems with the value of joint variables which are obtained from solving the IK are input data. Fig. 15 to Fig. 20 show the velocity and acceleration value of joints in three cases, respectively. The jerk values of the joints are shown in Fig. 21 to Fig. 25 for all 3 cases. Table 3 presents the maximum joint values of joints in all three cases.

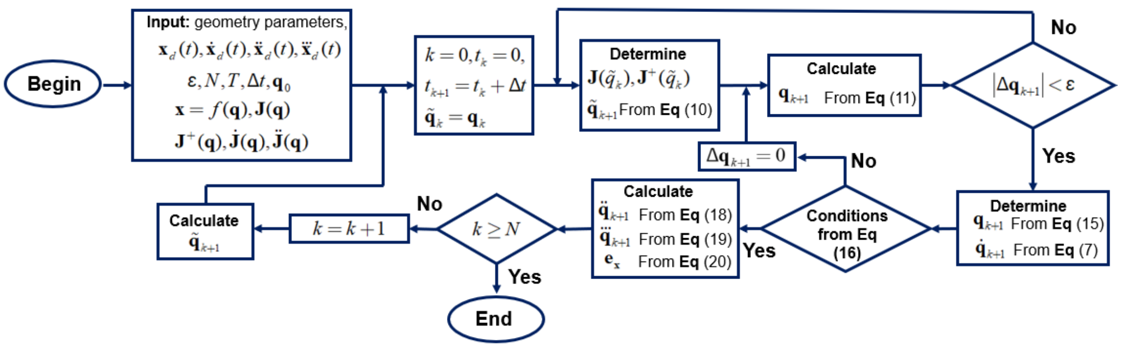

Fig. 2. Diagram of calculation steps

Case 1 (C1): The trajectory on OXY plane

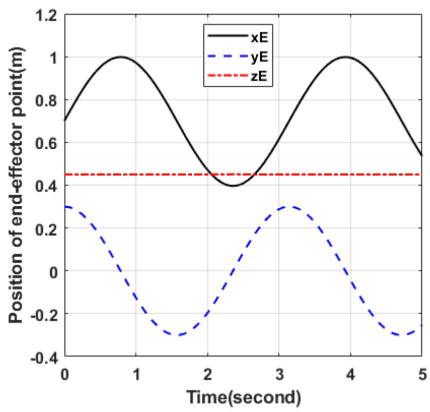

Fig. 3. Trajectory in C1

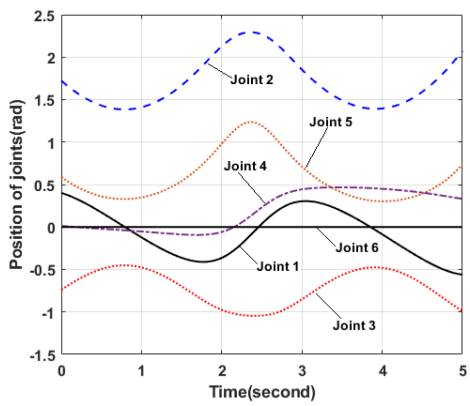

Fig. 4. Joint position in C1

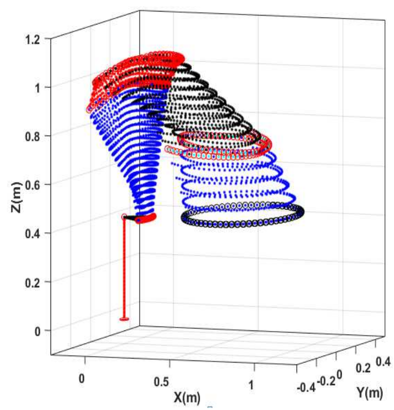

Fig. 5. Case 1

Case 2 (C2): The trajectory on OYZ plane

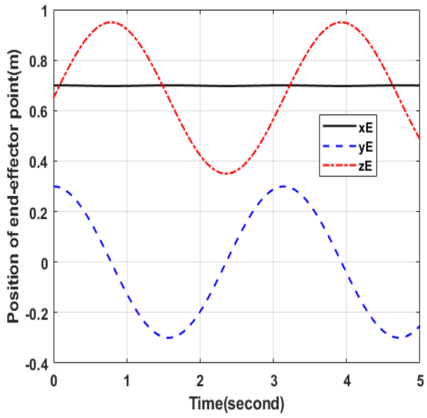

Fig. 6. Trajectory in C2

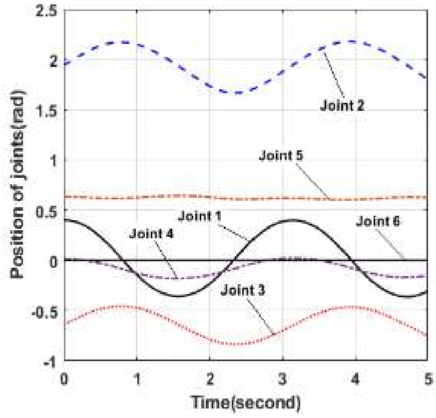

Fig. 7. Joint position in C2

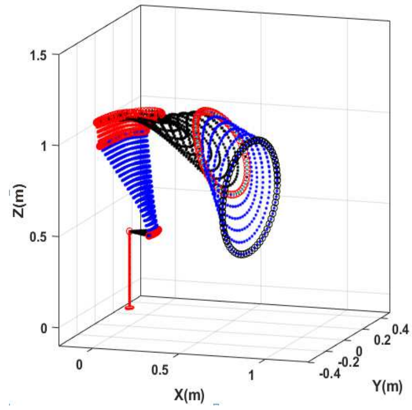

Fig. 8. Case 2

Case 3 (C3): The trajectory on OXZ plane

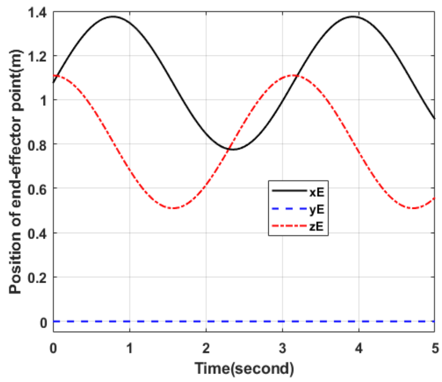

Fig. 9. Trajectory in C3

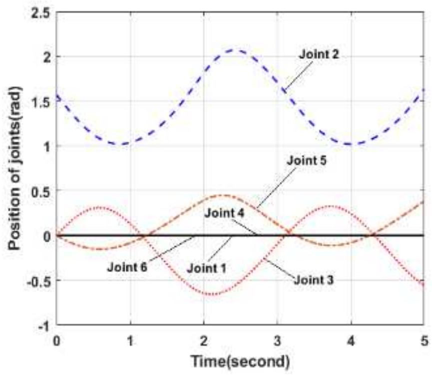

Fig. 10. Joint position in C3

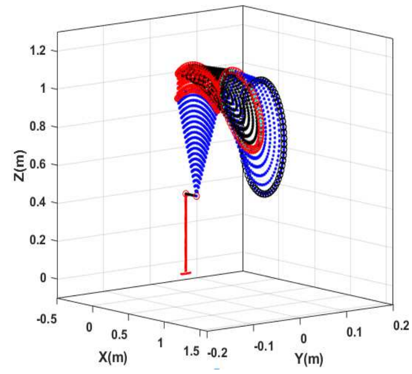

Fig. 11. Case 3

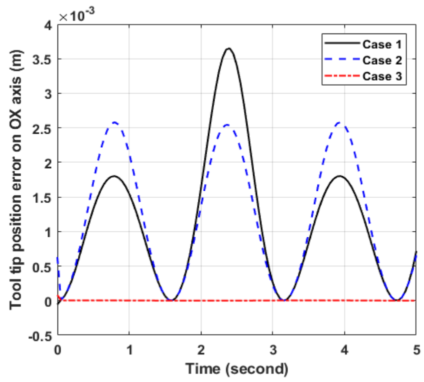

Fig. 12. Error position OX

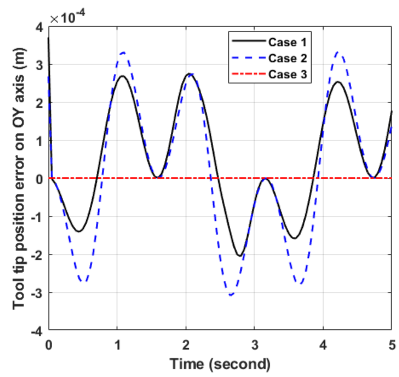

Fig. 13. Error position OY

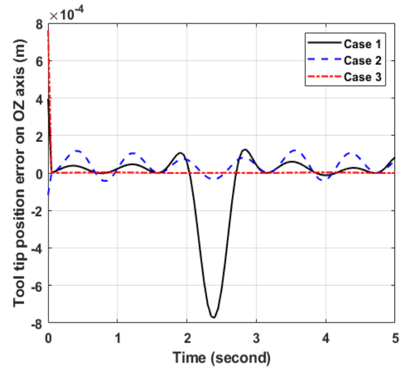

Fig. 14. Error position OZ

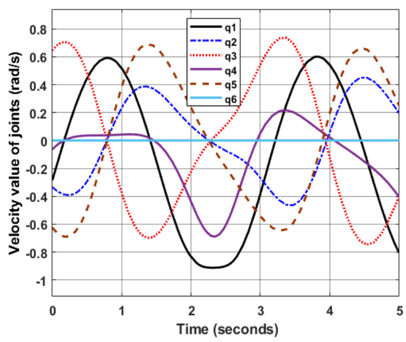

Fig. 15. Velocity value of joints in C1

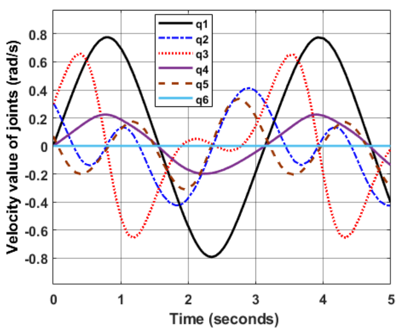

Fig. 16. Velocity value of joints in C2

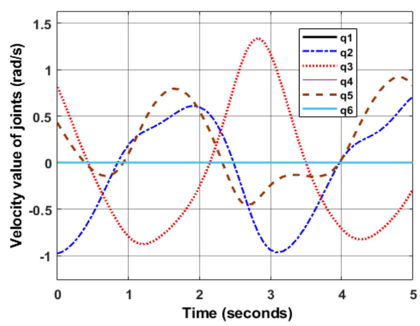

Fig. 17. Velocity value of joints in C3

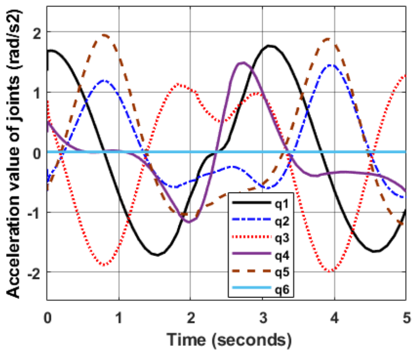

Fig. 18. Acceleration value of joints in C1

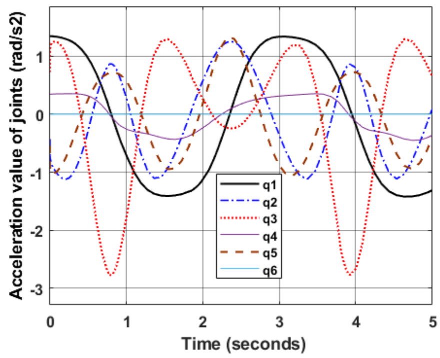

Fig. 19. Acceleration value of joints in C2

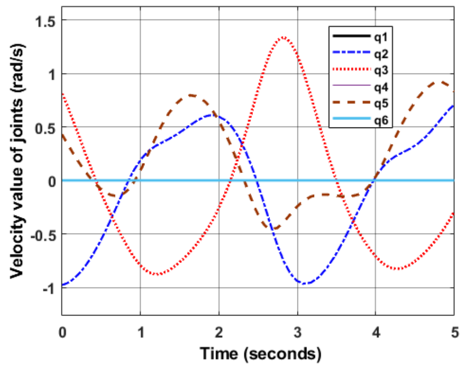

Fig. 20. Acceleration value of joints in C3

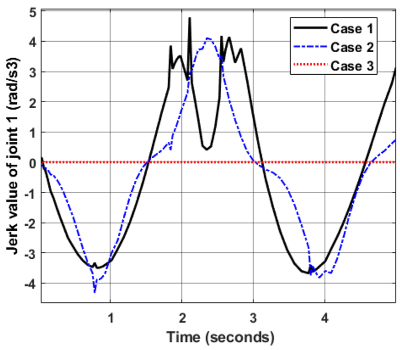

Fig. 21. Jerk joint 1

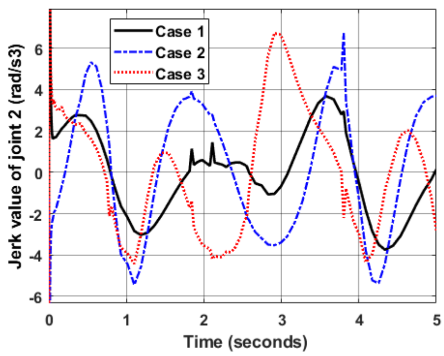

Fig. 22. Jerk joint 2

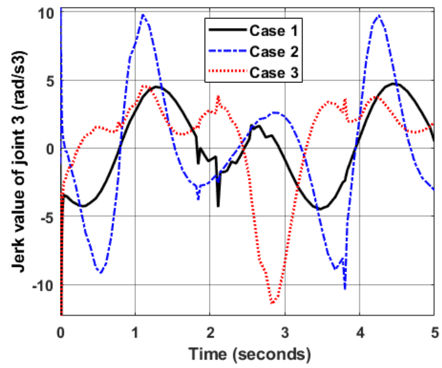

Fig. 23. Jerk joint 3

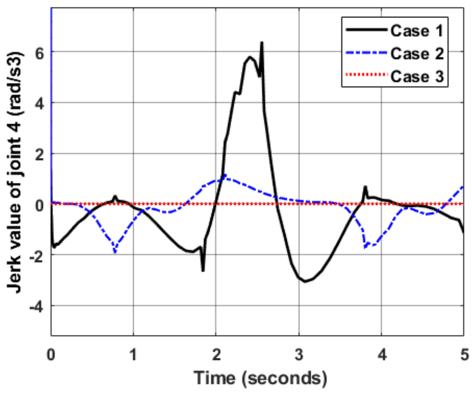

Fig. 24. Jerk joint 4

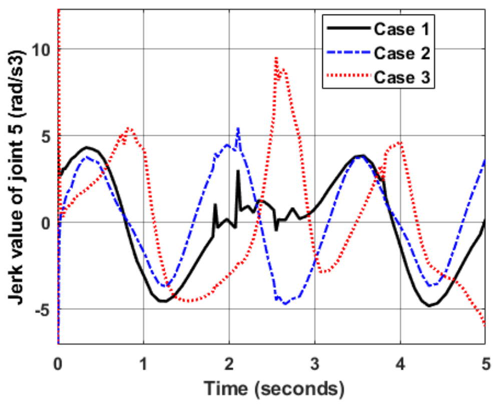

Fig. 25. Jerk joint 5

On the one hand, case 1 with the trajectory on the OXY plane gives the highest jerk in 3 cases. Jerk of joint 1 in case 1 is the largest with 4.95 (rad/s^3) and in case 3 is smallest with zero. This is quite understandable. Joint 1 in case 3 does not need to move because the EEP trajectory is in the XOZ plane. On the other hand, when the EEP point trajectory is close to the center of the robot, the jerk value changes continuously for a short time. The jerk value of joint 4 changed the most (6.4 rad/s^3) compared with case 2 (1.94 rad/s^3) and case 3 (0 rad/s^3). Case 3 also has a short-range of the EEP point trajectory near the robot center and also has the same jerky behavior as in case 1. The sudden change in jerk leads to increasing friction and temperature increase in the joints and it adversely affects the durability and longevity of the joints.

The jerk value of the joints 2, 3, and 5 in case 2 (6.73, 10.37, and 5.45 rad/s^3) and case 3 (6.73, 11.44, and 9.51 rad/s^3) is much greater than that of case 1 (3.69, 4.72 and 4.85 rad/s^3). This occurs when the EEP point trajectory gets too high or too low above the ground. The jerk of these joints in case 3 is the greatest due to the EEP point trajectory having the highest reach and closest to the ground.

Table 3. Maximum value of jerk at the joint

Joint jerk	Joint 1	Joint 2	Joint 3	Joint 4	Joint 5
Case 1	4.95	3.69	4.72	6.4	4.85
Case 2	4.32	6.73	10.37	1.94	5.45
Case 3	0	6.73	11.44	0	9.51

The value of joint 1 in case 1 (4.95 rad/s^3) and in case 2 (4.32 rad/s^3) have a continuous change value and are quite large, except in case 3 (0 rad/s^3). Joint 1 usually carries the maximum load due to having to support the entire weight of the robot. Therefore, the designer should limit the motion of joint 1 when designing the trajectory or minimize or avoid sudden changes in jerk value to improve joint life. According to this criterion, the EEP point trajectory is designed not too close to the robot center, preferably the trajectory lying on the XOZ plane (case 3) or the YOZ plane (case 2). Furthermore, this trajectory can be as high as the robot's maximum reach because the mass of the welding torch on the end-effector link is quite small but should not be too low above the ground. This also depends in part on the construction of the system to be welded.

From the obtained results, it can be seen that the trajectory design should restraint designing on the OXY plane (case 1) with the position of the EEP approaching the center of the robot because the jerk joints will tend to create vibrations on the links. The trajectory should tend to lie on the OXZ and OYZ planes (case 2). The best is the XOZ plane (case 3) because the jerk is quite uniform. This is of great importance in practical welding applications. The results of this study can be performed together with the designing of optimal welding trajectories taking into consideration joint jerky.

4. Conclusion

This paper has effectively applied the AGV algorithm to solve the IK of the redundant robots with 6-DOF. For each different trajectory change in the workspace, the kinematics characteristics of the robot such as the position, velocity, acceleration, and jerk of the joints are calculated to be within geometry limits, and ensure the minimum position error of the EEP. The jerk of the joints is determined to evaluate the effect of the change in their trajectory on them. The results showed that the jerks at joint 1 and joint 2 are large. With industrial robots fixed on the ground vertically, the trajectory in the OXY plane produces the greatest jerk compared to other planes. At the times when the EEP is closer to the center of the robot, joint jerk increases. On the other hand, the calculation results also show that trajectories are designed on the OXZ plane and OYZ plane and directed away from the robot's center, the jerk of the joint decreases. These will be good references for the design and optimization of the trajectory, optimize the robot's jerk and serve as the basis for reducing the actuator's system wear, improving longevity, and working efficiency. On the other hand, the research results show that the AGV algorithm is highly effective when applied to the special redundant robot systems with plenty of DOF combined with the trajectory optimization algorithms, the optimization of the feed rate of the torch.

Acknowledgments

The author is extremely grateful to anonymous reviewers for valuable comments that helped to improve this article.

Conflict of Interest

There are no potential conflicts of interest with respect to the research, authorship, and publication of this article.

Funding

The author received no financial support for the research, authorship, and publication of this article.

Nomenclature

$\mathbf{x}_d$	Desired path of the EEP [m]	$\mathbf{H}$	Homogeneous matrix in local coordinate frame
$\mathbf{q}(t)$	Generalized coordinate vector of Joint variables [rad]	$\mathbf{D}$	Homogeneous matrix in fixed coordinate frame
$\mathbf{J}(\mathbf{q})$	The Jacobian matrix		

References

[1] Homayoun, S., Configuration control of redundant manipulators: theory and implementation, *IEEE Transactions on Robotics and Automation, 5, 1989,* 472-490.

[2] Siciliano, B., Kinematic control of redundant robot manipulators: A tutorial, *Journal of Intelligent and Robotic Systems*, 3, 1990, 201-212.

[3] Chiaverini, S., Singularity robust task priority redundancy resolution for real time kinematic control of robot manipulators, *IEEE Transactions on Robotics and Automation*, 13, 1997, 398–410.

[4] Chiaverini, S., Oriono, G., Walker, I. D., *Kinematically Redundant Manipulators*, Springer Handbook of Robotics, Berlin, Heidenberg, 11, 2008, 245–268.

[5] Zlajpah. L., Petric, T., *Obstacle avoidance for redundant manipulators as control problem*, IntechOpen, 11, 2012, 203–230.

[6] Lian, S., Han, Y., Wang, Y., Bao, Y., Xiao, H., Li, X., Sun, N., Accelerating Inverse Kinematics for High-DOF Robots, *In: Proceedings of the 54th Annual Design Automation Conference, Austin,* USA, 2017.

[7] Yoshikawa, T., Dynamic manipulability of robot manipulators, *Journal of Robotic Systems*, 2, 1985, 113–124.

[8] Wampler, C. W., Manipulator inverse kinematic solutions based on vector formulations and damped least squares methods, *IEEE Transactions on Systems, Man, and Cybernetics,* 16, 1986, 93–101.

[9] Wang, L. C. T., Chen, C. C., A combined optimization method for solving the inverse kinematics problem of mechanical manipulators, *IEEE Transactions on Robotics and Automation, 7,* 1991, 489–499.

[10] Zhao, J., Badler, N. I., Inverse kinematics positioning using nonlinear programming for highly articulated figures, *ACM Transactions on Graphics*, 13, 1994, 313–336.

[11] Sciavicco, L., Siciliano, B., A Solution Algorithm to the Inverse Kinematic Problem for Redundant Manipulators, *Journal of Robotics and Automation*, 4, 1988, 403-410.

[12] Antonelli, G., Chiaverini, S., Fusco, G., Kinematic control of redundant manipulators with online end-effector path tracking capability under velocity and acceleration constraints, *In: IFAC Robot Control, Austria*, 2000, 183-188.

[13] Wang, J., Li, Y., Zhao, X., Inverse kinematics and control of a 7 DOF redundant manipulator based on the closed loop algorithm, *International Journal of Advanced Robotics Systems*, 7, 2010, 1 -10.

[14] My, C. A., Bien, D. X., Tung, H. B., Hieu, L. C., Cong, N. V., Hieu, T. V., Inverse kinematic control algorithm for a welding robot-positioner system to trace a 3D complex curve, *In: International Conference on Advanced Technologies for Communications*, Hanoi, Vietnam, 2019, 319-323.

[15] Aguilar, O. A., Huegel, J. C., Inverse Kinematics Solution for Robotic Manipulators Using a CUDA-Based Parallel Genetic Algorithms, *Mexican International Conference on Artificial Intelligence,* 1, 2011, 490-503.

[16] Bingul, Z., Ertunc, H. M., Oysu, C., Comparison of inverse kinematics solutions using neural network for 6R robot manipulator with offset, *Computational Intelligence Methods and Applications*, 2005, 1–5.

[17] Feng, Y., Yaonan, W., Yimin, Y., Inverse kinematics solution for robot manipulator based on Neural Network under joint subspace, *International Journal of Computer and Communications*, 7, 2012, 459-472.

[18] Xu, H. L., Xie, X. R., Zhuang, J., Wang, S. A., Global time-energy optimal planning of industrial robot trajectories, *Chinese Journal of Mechanical Engineering*, 46, 2010, 19-25.

[19] Osgouie, K. G., Gard, B., Using the matrix method to compute the degrees of freedom of mechanism, *Journal of Applied and Computational Mechanics*, 3(3), 2017, 158 – 170.

[20] Alessandro, G., Zanotto, V., A technique for time-jerk optimal planning of robot trajectories, *Robotics and Computer-Integrated Manufacturing*, 24, 2008, 415-426.

[21] Palleschi, A., Garabini, M., Caporale, D., Pallottino, L., Time-Optimal Path Tracking for Jerk Controlled Robots, *IEEE Robotics and Automation Letters*, 2019, 1-8.

[22] Pierre-Jean, B., Richard, B., Pierre, B., Eric, D., Influence of a Jerk Controlled Movement Law on the Vibratory Behaviour of High-Dynamics Systems, *Journal of Intelligent & Robotic Systems*, 42, 2005, 275-293.

[23] Friedrich, L., Michael, S., Trajectory Generation for Immediate Path-Accurate Jerk-Limited Stopping of Industrial Robots, *Proceeding in International Conference on Robotics and Automation (ICRA)*, Seattle, WA, USA, 2015.

[24] Piazzi, A., Visioli, A., Global Minimum-Jerk Trajectory Planning of Robot Manipulators, *IEEE Transactions on Industrial Electronics*, 47, 2000, 140-149.

[25] Gabor, V., Bela, L., Shahram, P., Real-time optimized robot trajectory planning with jerk, *IFAC Robot Control*, Wroclaw, Poland, 2003, 265-270.

[26] Lin, H., Liu, Y., Minimum-Jerk Robot Joint Trajectory Using Particle Swarm Optimization, *In: First International Conference on Robot, Vision and Signal Processing*, 2011, 118-121.

[27] Vanni, Z., Alessandro, G., Albano, L., Paolo, B., Renato, V., Experimental Validation of Minimum Time-jerk Algorithms for Industrial Robots, *Journal of Intelligent Robot Systems*, 64, 2011, 197–219.

[28] Rubio, F., Valero, F., Suñer, J. L., Cuadrado, J. I., Optimal time trajectories for industrial robots with torque, power, jerk and energy consumed constraints, *Industrial Robot: An International Journal*, 29, 2012, 92-100.

[29] Chengkai, D., Sylvain, L., Kai-Ming, Y., Jo, M. P. G., Charlie, C., Wang, L., Planning Jerk-Optimized Trajectory with Discrete-Time Constraints for Redundant Robots, *IEEE Transactions on Automation Science and Engineering*, 17, 2020, 1711-1724.

[30] Kazem, K., Zhaoyu, W., Global versus Local Optimization in Redundancy Resolution of Robotic Manipulators, *The International Journal of Robotics Research*, 7, 1988, 1-10.

[31] Spong, M. W., Hutchinson, Vidyasagar, S. M., *Robot modeling and Control*, First edition, New York, USA, John Wiley and Sons, 2001.

[32] Philip, F., *Minimum Jerk Trajectory Planning for Trajectory Constrained Redundant Robots*, Ph.D. Thesis, School of Engineering and Applied Science, Department of Electrical and Systems Engineering, Washington University in St. Louis, Saint Louis, Missouri, USA, 2012.

[33] Ying, W., Xiaogang, Y., Liangyu, H., Hongzhou, T., Yunong, Z., Inverse-Free Solution of ZIGI Type to Acceleration-Level Inverse Kinematics of Redundant Robot Manipulators, *7th International Conference on Advanced Computational Intelligence Mount* Wuyi, Fujian, China; March 27-29, 2015, 57-62.

[34] Macfarlane, S., Croft, E. A., Jerk-Bounded Manipulator Trajectory Planning: Design for Real-Time Applications, *IEEE Transactions on Robotics and Automation*, 1, 2003, 42-52.

[35] Vass, G., Lantos, B., Payandeh, S., Real-time optimized robot trajectory planning with jerk, *In: IFAC Robot Control, Wroclaw, Poland*, 2003, 265-270.

[36] Zhao, R., Sidobre, D., Trajectory Smoothing using Jerk Bounded Shortcuts for Service Manipulator Robots, *In: International Conference on Intelligent Robots and Systems (IROS)*, 2015, 4929-4934.

[37] Lu, S., Zhao, J., Jiang, L., Liu, H., Solving the Time-Jerk Optimal Trajectory Planning Problem of a Robot Using Augmented Lagrange Constrained Particle Swarm Optimization, *Mathematical Problems in Engineering,* 2017, 1-11.

[38] Dai, C., Lefebvre, S., Yu, K., Geraed, J. M. P., Wang, C. C. L., Planning Jerk-Optimized Trajectory with Discrete-Time Constraints for Redundant Robots, *IEEE Transactions on Automation Science and Engineering*, 2020, 1-14.

[39] Cao, Z. Y., Wang, H., Wu, W. R., Xie, H. J., Time-jerk optimal trajectory planning of shotcrete manipulators, *Journal of Central South University*, 44, 2013, 114-121.

[40] Zhong, G. L., Kobayashi, Y., Emaru, T., Minimum time-jerk trajectory generation for a mobile articulated manipulator, *Journal of the Chinese Society of Mechanical Engineers,* 35, 2014, 287-296.

[41] Liu, F., Lin, F., Time-jerk optimal planning of industrial robot trajectories, *International Journal Robotics Automation,* 31, 2016, 1-7.

[42] FD-V8 robot from https://www.daihen-usa.com/product/fd-v8-robot-6kg-payload-1-4m-reach/ (Access: August 2020).

[43] Khang, N. V., Dien, N. P., Vinh, N. V., Nam, T. H., Inverse kinematic and dynamic analysis of redundant measuring manipulator BKHN-MCX-04, *Vietnam Journal of Mechanics,* 32, 2010, 15-26.

[44] Raunhardt, D., Boulic, R., Progressive clamping, *IEEE International Conference on Robotics and Automation (ICRA)*, 2007, 4414–4419.

ORCID iD

Xuan Bien Duong https://orcid.org/0000-0001-7380-8551

How to cite this article: Duong X.B. On the Effect of the End-effector Point Trajectory on the Joint Jerk of the Redundant Manipulators, *J. Appl. Comput. Mech.*, 7(3), 2021, 1575–1582. https://doi.org/10.22055/JACM.2021.35350.2635